



REVIEW

Optical Coherence Tomography Angiography: A 2023 Focused Update on Age-Related Macular Degeneration

Beatrice Tombolini · Emanuele Crincoli · Riccardo Sacconi ·
Marco Battista · Federico Fantaguzzi · Andrea Servillo ·
Francesco Bandello · Giuseppe Querques

Received: September 14, 2023 / Accepted: December 5, 2023 / Published online: January 5, 2024
© The Author(s) 2024

ABSTRACT

Optical coherence tomography angiography (OCTA) has extensively enhanced our comprehension of eye microcirculation and of its associated diseases. In this narrative review, we explored the key concepts behind OCTA, as well as the most recent evidence in the pathophysiology of age-related macular degeneration (AMD) made possible by OCTA. These recommendations were updated since the publication in 2020, and are targeted for 2023. Importantly, as a future perspective in OCTA technology, we will discuss how artificial intelligence has been applied to OCTA, with a particular emphasis on its application to AMD study.

Keywords: Optical coherence tomography angiography; 3D OCTA; Age-related macular degeneration; Non-exudative macular neovascularization; Quiescent neovascularization; Subclinical neovascularization; Geographic atrophy; Type 3 macular neovascularization; Artificial intelligence

Key Summary Points

Optical coherence tomography angiography (OCTA) has drastically changed the approach to diagnosis and treatment in ophthalmology.

In this narrative review, the key concepts underlying OCTA technology will be covered, from how to acquire quantitative metrics to OCTA limitations that should be properly considered.

A particular focus on OCTA application in age-related macular degeneration will be undertaken, with an overview of the most recent evidence.

Artificial intelligence and other novel OCTA applications, such as tridimensional visualization, will also be discussed.

B. Tombolini · E. Crincoli · R. Sacconi ·
M. Battista · F. Fantaguzzi · A. Servillo ·
F. Bandello · G. Querques (✉)
School of Medicine, Vita-Salute San Raffaele
University, Milan, Italy
e-mail: querques.giuseppe@hsr.it;
giuseppe.querques@hotmail.it

B. Tombolini · E. Crincoli · R. Sacconi ·
M. Battista · F. Fantaguzzi · A. Servillo ·
F. Bandello · G. Querques
Division of Head and Neck, Ophthalmology Unit,
Department of Ophthalmology, IRCCS San Raffaele
Scientific Institute, Via Olgettina 60, 20132 Milan,
Italy

INTRODUCTION

Optical coherence tomography angiography (OCTA) has revolutionized the diagnosis and therapeutic management in ophthalmology. The basic principle underlying this noninvasive technique is that the rapid acquisition of scans at the same location can detect the flow of a natural “dye,” blood, inside ocular vessels [1–8].

As a result, our understanding of the anatomic distribution of retinal and choroidal vasculatures has been considerably improved. Inner and middle retina have been shown to be nourished by four capillary plexuses. In detail, the superficial capillary plexus (SCP) provides the retinal nerve fiber and ganglion cell layers, while the inner nuclear layer is vascularized by the medium (or intermediate) capillary plexus (MCP) and by the deep capillary plexus (DCP). Notably, a circular avascular area known as the foveal avascular zone (FAZ) has been described as the anastomosis of these three capillary plexus at the parafoveal location [9]. Finally, the radial peripapillary capillary plexus (RPCP), which feeds the innermost portion of the peripapillary nerve fiber layer, is the fourth retinal plexus [9]. In contrast, the choroid consists of three vessel layers of increasing sizes, the innermost of which is the choriocapillaris (CC) and supplies outer retina.

Despite its significant advantages, OCTA has not been employed in clinical practice as a gold standard diagnostic technique yet, with the exception of contraindication to conventional dye-based angiography [fluorescein angiography (FAG) and indocyanine green angiography (ICGA)]. Therefore, OCTA is still regarded as a complementary approach to FAG and ICGA for the diagnosis of neovascular age-related macular degeneration (nAMD). Additionally, AMD screening using self-assessment tools such as the Amsler grid [10] and mobile medical applications (e.g., OdySight Care) [11] showed detection rates that were lower than those of tomographic methods.

METHODS

In this narrative review, we will briefly discuss the fundamental concepts behind OCTA technology, and provide an overview of the most recent evidence concerning OCTA application in AMD.

A PubMed search was conducted by using the following keywords: “optical coherence tomography angiography,” “OCTA,” “2D OCTA,” “3D OCTA,” “age-related macular degeneration,” “non-exudative macular neovascularization,” “quiescent macular neovascularization,” “subclinical macular neovascularization,” “geographic atrophy,” “type 3 macular neovascularization,” and “artificial intelligence.” Each English-language study that was published up through August 2023 was reviewed and, if appropriate, was included in the current narrative review.

This article is based on previously conducted studies and does not contain any new studies with human participants or animals performed by any of the authors. Thus, no approval from local ethics committee was required.

OPTICAL COHERENCE TOMOGRAPHY ANGIOGRAPHY (OCTA)’S TECHNICAL ASPECTS

Pearls of OCTA’s Function

OCTA scans are equivalent to signal variation in repeated structural optical coherence tomography (OCT) B-scans at the same location (decorrelation signal) caused by moving structures within a stationary background, namely erythrocytes inside blood vessels (motion contrast) [7, 8]. OCTA instruments acquire a variable number of repeated B-scan (usually 2–4 scans for commercial instruments, or even more for research machines). This difference depends on the type of OCTA device, including swept-source OCTA (SS-OCTA) and spectral-domain OCTA (SD-OCTA). Notable differentiations between SS-OCTA and SD-OCTA include quicker scan acquisition rates (100,000–400,00 A-scans/s versus 27,000–70,000 A-scans/s,

respectively), deeper penetration (wavelength 1050 nm versus wavelength 840 nm, respectively), and improved choroid visibility [6]. Another crucial OCTA variable is the “interscan time,” which indicates the time delay between two consecutive B-scans at the same position. Since each B-scan is composed of several A-scans, interscan time is conditioned by A-scan rate and sampling density (number of A-scans/unit distance), and by B-scan dimension (e.g., length). Thus, slower A-scan rates will imply longer interscan times, with higher sensitivity to slow motion, but also more frequent motion artifacts (see the paragraph “2D OCTA’s pitfalls affecting AMD evaluation” below). Interestingly, OCTA devices cannot detect flow that is slower than a motion threshold defined by interscan time and background noise (“undetectable flow”). Notably, perfusion loss may be secondary to OCTA insensitivity, rather than a real lack of flow. In parallel, OCTA also displays a dynamic sensitivity to detect flow variations (“saturation limit”) over which the signal is “saturated” and no flow differences are discerned, as occurs in the case of shorter interscan times [1]. Variable interscan time analysis (VISTA) is an innovative approach to overwhelm this limit of OCTA of not quantifying flow velocity. In fact, VISTA technique may roughly revealed flow alterations by comparing differences in flow signals or motion after the variation of interscan times [2]. However, exact flow velocity cannot be determined even by this innovative OCTA approach [1]. Different platforms currently use a variety of OCTA algorithms. For instance, the amplitude algorithm and phase algorithm evaluate signal variation in amplitude and phase, respectively. More recently, the split-spectrum amplitude decorrelation algorithm (SSADA) employs amplitude information, while the optical micro-angiography (OMAG) technique combines both phase and amplitude data. Another algorithm is OCT angiography ratio analysis (OCTARA), which is more perceptive to low blood flow [12].

TWO-DIMENSIONAL (2D) OCTA VISUALIZATION

OCTA data can be represented as both two-dimensional (2D) B-scan and en-face images, as well as three-dimensional (3D) images. B-scan corresponds to a pseudo-color overlay on a cross-sectional OCT. En-face scan represents a segmentation image with a projection of the flow data at a given level. Slabs are the volumetric section that is defined by two topographic surfaces [3, 5].

Interestingly, en-face images could be elaborated, undergoing a binarization and/or skeletonization processes to acquire quantitative metrics of retinal and choroidal vessels. In detail, binarized images are defined by a threshold from grayscale values, which determines whether pixels should be presented as white (or black) depending on whether pixels’ value is higher or lower than this threshold. Thus, binarization leads to isolate retinal vessels from the background [2, 3]. Different binarization thresholdings have been proposed, although there is still no consensus [13]. Then, the binarized image may undergo a skeletonization process to be represented as traces of one pixel in width [14].

So far, several OCTA quantitative metrics have been introduced for retinal microvasculature [3, 5], although this narrative review did not mean to report them. However, these metrics proved to lack consistency due to several aspects. Measurement results proved to vary on the basis of the OCTA device, scan size, and binarization thresholding approaches, thus the results are not homogeneous [15–18]. Furthermore, additional variability factors are brightness and/or contrast changes before the binarization process since no consensus on the most effective technique has been reached.

CC perfusion quantification requires also a binarization from OCTA en-face images. In detail, this procedure aims to separate the bright region representing the choriocapillaris’s preserved flow from the so-called flow voids or signal voids, which constitute dark areas of vascular dropout or flow below decorrelation threshold, respectively [2, 19, 20]. Regardless of

the introduction of several CC binarization approaches, recently Phansalkar's method has been proposed as the reference procedure [21]. For further details, please consult our previous narrative reviews about this topic [3, 5].

2D OCTA'S PITFALLS AFFECTING AMD EVALUATION

Optical coherence tomography angiography has overtaken some limitations of invasive angiographic techniques, which are still regarded as the standard procedures to assess ocular microvasculature except in cases where traditional angiography is contraindicated (e.g., severe dye allergy) [22]. Indeed, OCTA is a dye-free noninvasive rapid approach that separately displays each ocular vascular network, also including MCP, DCP, and CC, in contrast to previous techniques [2, 23]. However, it is clear that this method may be affected by several limitations, some of which are particularly relevant in the evaluation of AMD eyes. For instance, an increase in background noise (e.g., media opacities) may interfere with the detection of a low-strength signal [24]. Artifacts have been associated to patient's movement (e.g., blinking, eye displacement), whose impact have been decreased by eye tracking systems [25]. However, stretch artifacts, quilting, and vessel doubling are examples of other motion artifacts that are secondary to software-corrected eye movements, as well [26]. Another OCTA artifact is the segmentation error that results from the flattening of data in a segmented two-dimensional volume [1–3]. Many devices can correct this artifact by manual correction of segmentation errors and throughout averaging of multiple B-scans [25, 27, 28]. Recently, the deep learning (DL)-based algorithm has improved segmentation of OCTA data (see paragraph "4.4 Future direction: artificial intelligence" below) [29]. Furthermore, projection artifacts may affect the visualization of vascular layers if superficial vessels are falsely recognized in deep layers in absence of true flow, especially when they are located close to tissues with high back scattering [such as retinal pigment epithelium (RPE)]. In cross-sectional scans, projection

artifacts also result in "tails" on vessels (decorrelation tails). To reduce these artifacts, slab subtraction may be applied by removing the signal in superficial plexuses from angiograms of deeper tissue. However, if the artifact signal aligns with true flow signal, it can be eliminated as well. Cross-sectional images cannot be subjected to slab subtraction. Several voxel-by-voxel-based post-processing algorithms, such as projection-resolved OCTA (PR-OCTA) and signal attenuation-compensated projection-resolved OCTA (sacPR-OCTA), have been used for OCTA to remove projection artifacts. The rationale for PR-OCTA technique is that the reflectance-normalized signal in projection artifacts is lower than the real flow one in adjacent voxels. The algorithm preserves the flow values at the sequentially higher peaks (in situ flow) over each A-line and suppresses the rest to background level using structural OCT signal to weigh the flow signal in the OCTA volume [30]. However, PR-OCTA may underestimate flow signal, particularly in low-quality slab. On the contrary, sacPR-OCTA also took into account the corresponding signal attenuation with distance from true flow signal, and improved true flow signal beneath larger arteries and in the shadow zone [31].

Shadowing artifacts can occur if OCT signal is attenuated or blocked at level of MCP, DCP, or CC, due to an obstacle to beam transmission (e.g., vitreous opacities, hemorrhage, and drusen) [1]. In conclusion, the impact of these artifacts can be mostly mitigated by software (automation of vessel segmentation, algorithms, including DL-based one), or hardware approaches, although there is a variable influence on qualitative/quantitative analyses and possible artifacts related to these correction procedures [2, 32, 33]. Another OCTA limitation is the still inaccurate visualization of Sattler and Haller's layers because of scattering effect by RPE and CC vessels, and slow blood flow [34]. With the advent of SS-OCTA technology, this latter restriction has been partially overcome [35, 36]. Deep choroidal imaging, however, mostly relies on structural OCT rather than angiography OCT. The development of enhanced-depth imaging (EDI) SD-OCT and SS-OCT technology has particularly contributed to

the inclusion of choroidal analysis into standard clinical practice [34].

Furthermore, OCTA has a narrow field of view that only includes the posterior pole region, despite wide-field SS-OCTA, with its 50–80 degree retinal surface viewing, having just been introduced, showing promising clinical uses (e.g., retinal vascular disorders). Finally, this imaging examination does not provide functional information (e.g., fluorescein leakage), in contrast to conventional angiographic exams [12].

THREE-DIMENSIONAL (3D) OCTA VISUALIZATION

Three-dimensional volume-rendering OCTA has recently been recognized as a useful tool for qualitative and quantitative assessment of ocular microvasculature. To create 3D images, various semi-automated algorithms have been proposed, including one developed by our group [37–40]. In detail, after the removal of projection artifacts (ARI network projection removal algorithm, Zeiss), these data are imported to Fiji (Image J, National Institutes of Health, Bethesda, USA). Through this software, OCTA scan is re-oriented in space (“rotation analysis”) with the first dimension corresponding to axial direction, whereas the second and third dimensions match the horizontal and vertical directions, respectively. Finally, the 3D Viewer plugin provides the rotational 3D visualization (Image J, software version 2.0.0, National Institutes of Health, Bethesda, USA). Although the two-dimensional approach remains the gold standard OCTA visualization, volume-rendering scan overcame some 2D limitations. The three-dimensional image is independent on data segmentation and on flattening of flow, as compared with the two-dimensional scan. Furthermore, no overlapping anatomy or vessels’ foreshortening may affect this OCTA visualization. Consequently, 3D modality was found to be the most effective modality to detect findings, such as diabetic microaneurysms, diabetic macular ischemia, and type 3 macular neovascularization (MNV), that could be oriented on the three dimensions

[37–41]. Interestingly, our group confirmed histologic evidence that type 3 MNV is a retina–retinal vascular anastomosis, also providing new insight into type 3 pathogenesis (Fig. 1). Since some of these lesions did not reach sub-RPE space, different stages constituting immature (or nascent) lesions may coexist. Furthermore, similar to Müller cells, which are known to direct its implant, type 3 neovascularization displayed an oblique orientation toward the outer retina. Finally, due to an accurate recognition of the lesion’s branching vasculature, 3D visualization demonstrated a greater detection rate of this MNV subtype than two-dimensional technique [38]. The results of our subsequent research showed that type 3 MNV activity corresponds to the response to anti-vascular endothelial growth factor (VEGF) injections, but not with a full recovery following intravitreal therapy. Therefore, this evidence supported the use of this OCTA visualization for evaluating the effectiveness of intravitreal therapy, as well [40]. However, rotational 3D OCTA images should be viewed cautiously due to some limitations intrinsic to OCTA devices, including projection artifacts and the inability to discern flow under a detectable threshold [38].

Furthermore, our group developed quantitative metrics of 3D OCTA scans, including:

- 3D vascular volume, indicating the total vascular volume of a retinal region of interest.
- 3D perfusion density, expressing the relative perfusion on the basis of neuroretina volume.

These variables showed an excellent reliability and intrasession repeatability in patients affected by diabetic retinopathy and healthy subjects, in comparison to 2D OCTA parameters [42].

OCTA UPDATES ON AGE-RELATED MACULAR DEGENERATION

Age-related macular degeneration has been thoroughly studied with OCTA due to its accurate visualization of deep capillary plexus and

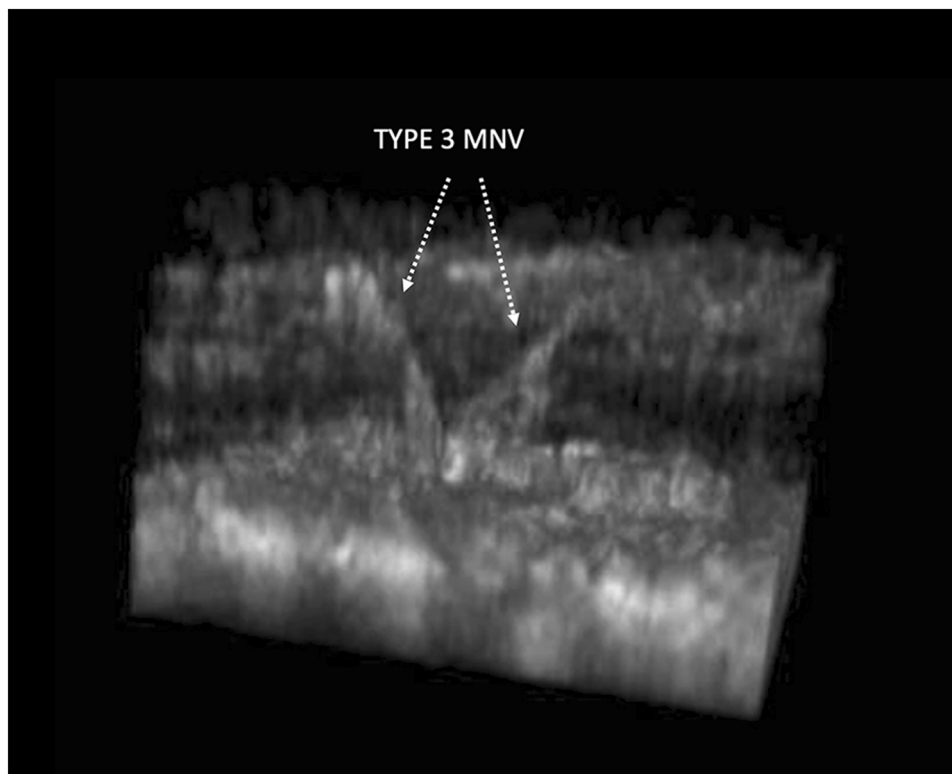


Fig. 1 Three-dimensional optical coherence tomography angiography of a 80-years-old male patient affected by type 3 MNV showing two neovessels connecting the deep

capillary plexus to the RPE/sub-RPE space. *MNV* macular neovascularization, *RPE* retinal pigment epithelium

choriocapillaris. In this section, the current narrative review will be focused on the most recent insights into the pathophysiology of AMD.

OCTA AND SUBRETINAL DEPOSITS IN INTERMEDIATE AMD

OCTA have been employed in intermediate AMD to investigate the impact of subretinal deposits on ocular microvasculature, although with controversial evidence. Kalaw and associates found a significant reduction of macular vessel density (VD) at the DCP level in eyes with reticular pseudodrusen (RPD), and a corresponding thinning of inner and outer retina layers, as compared with soft-drusen-only patients [43]. Conversely, another group correlated a similar retinal thinning to a significantly increased macular DCP VDs in a RPD cohort, suggesting that reticular pseudodrusen may

induce hypoxia, and thus a higher vascular request [44]. In parallel, Li and colleagues focused on the choroidal features of intermediate AMD. Interestingly, RPD eyes showed higher macular CC FD, with lower choriocapillaris and reduced mean choroidal thickness than in healthy and soft drusen patients [45]. Therefore, RPD development in AMD could be the result of a choroidal perfusion impairment, as also proved by other similar workgroups [45, 46]. On the contrary, Wu et al. reported no relevant differences in CC FD and mean choroidal thickness, suggesting that RPD did not alter vascular parameters in intermediate AMD [47].

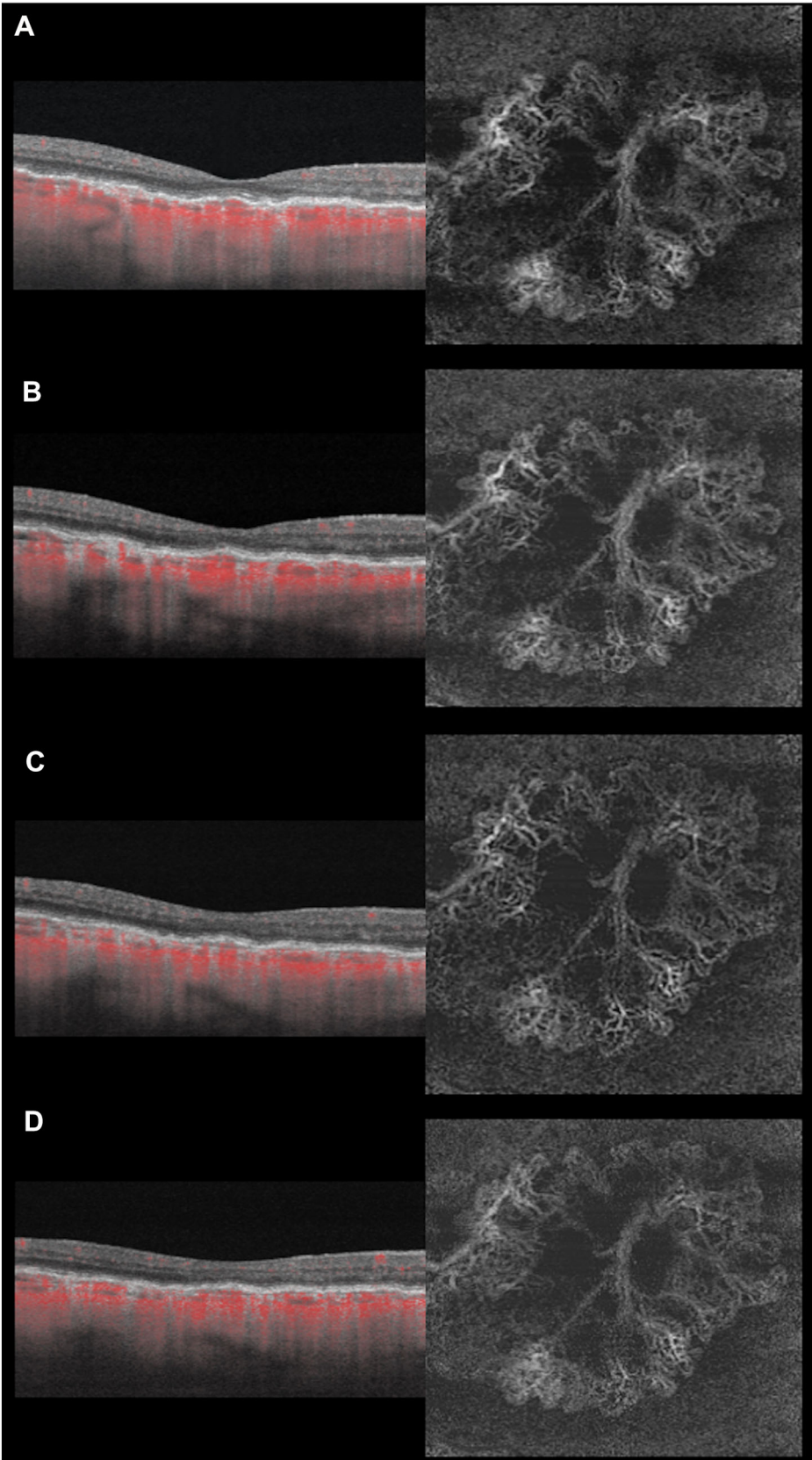
OCTA AND NON-EXUDATIVE MACULAR NEOVASCULARIZATION (NE-MNV)

Non-exudative MNV (NE-MNV) originally designated a treatment-naïve macular

neovascularization with no exudative signs (“inactive” MNV) on repeated OCT B-scans for at least 6 months [48]. Subsequently, these lesions were labeled as “quiescent” or “subclinical.” Briefly, if this phenotype remains inactive for 6 months, it was categorized as “quiescent.” On the contrary, “subclinical” MNV was defined as an ex-novo neovascular network with no minimum follow-up or period without exudation. As a result, this latter form actually denoted a pre-exudative stage. (Fig. 2A–D). However, the use of the term “non-exudative MNV” was encouraged, as there is currently no terminology consensus, and this definition included a spectrum of diseases with different phenotypes (quiescent versus subclinical) [49].

Literature validating OCTA as an elective method for NE-MNV diagnosis is continuously growing. Interestingly, when detection rates of NE-MNV were compared between OCTA and conventional angiographic modalities, OCTA identified the same number of lesions as ICGA, but FAG found none [50]. Conversely, Stattin et al. reported higher OCTA accuracy and smaller NE-MNV area size than indocyanine angiography (80% versus 11%, respectively), with combined OCTA en-face and B-scans showing the highest detection rate (50%) [51]. However, the diagnostic performance of OCT angiography may be influenced by the type of slab used (en-face versus cross-sectional) and kind of segmentation (manual customized versus automatic). In detail, automatic cross-sectional OCTA showed the greatest sensitivity (84%) in detecting MNV, thus being the preferred choice for these lesions. On the contrary, manual segmentation by expert retinal specialists may increase the performance of OCTA en-face slab [52]. Different groups tried to identify predictors of development, growth, and exudation of NE-MNV through OCTA [53–58]. An innovative study from Fragiotta and colleagues evaluated the role of subretinal lipid globules (SLG) as a biomarker of development and growth of NE-MNV. This finding corresponds on SD-OCT to a round hyporeflective lesion located between the ellipsoid zone and RPE/Bruch’s membrane complex. Notably, SLG may be regarded as a risk factor for NE-MNV development since the identification of non-

exudative MNV was higher in SLG cohort than in eyes without them (93.3% versus 18.4%, respectively). Furthermore, SLG was correlated to larger MNV size area and faster NE-MNV growth, being a growth predictor, as well. However, the rate of conversion from non-exudative to exudative state was similar, regardless of the presence of SLG [57]. Concerning the role of NE-MNV as a predictor of exudation, the growth in size of the neovascular lesion appeared to be a relevant activation biomarker [54], although both inactive and active MNV clearly increases over time [59]. However, Querques and colleagues demonstrated that NE-MNV grows with different rates, thus classifying it as it follows: “persistently quiescent” NE-MNV, which did not develop signs of exudation; “long-term activated” NE-MNV, which showed exudative signs after 6 months; and “short-term activated” (or “subclinical”) NE-MNV, which exudated within 6 months. Interestingly, this analysis found that “persistently quiescent” and “long-term activated” groups did not differ in anatomical features and lacked of activation biomarkers. On the contrary, “short-term activators” NE-MNV displayed a higher baseline perfusion density (PD), and thus a faster increase in MNV area than other phenotypes [53]. In fact, the elevated PD may correspond to a higher number of capillaries. Thus, Sacconi et al. speculated that the origin of “short-term activator” NE-MNV is driven mainly by angiogenesis, which results in a growth of neovascular network and an increased PD due to elevated proliferation of new capillaries. Consequently, it is probable that this “subclinical” phenotype actually constitutes a pre-exudative stage in the genesis of exudative MNV. Conversely, the other groups may be the result of arteriogenesis that is characterized by dilatation of preexisting vessels with no capillaries sprouting, and thus by a low PD on OCTA. As a result, a baseline high vascular density may predict exudation in NE-MNV [53, 55]. Maltsev et al. suggested the involvement of a more preserved RPE in comparison to active MNV as a further explanation for increased VD in non-exudative lesions. [60]. Similarly, an interesting study from Wang et al. reported that a growth of at least 50% of NE-MNV area within 1 year of follow up may



◀**Fig. 2 (A–D)** Optical coherence tomography angiography of a 75-year-old male patient affected by non-exudative quiescent type 1 macular neovascularization. **(A)** Baseline OCTA B-scan (left) and en-face (right) at RPE level. Confluent DEPs present detectable flow, representing non-exudative type 1 MNV. **(B–D)** OCTA B-scan (left) and en-face (right) at RPE level after 6 months **(B)**, 12 months **(C)**, and 18 months **(D)** did not detect activation signs, thus showing non-exudative quiescent MNV. *MNV* macular neovascularization, *RPE* retinal pigment epithelium, *DEP* pigment epithelium detachments, *OCTA* optical coherence tomography angiography

constitute a risk factor for exudation and for an earlier activation than eyes with stable MNV [58]. Furthermore, a branching pattern of the MNV and the hypointense ring surrounding the lesion (“dark halo”) have been identified as activity biomarkers, as well [56]. The validity of any of these OCTA biomarkers as precise predictors of exudative activity has not been established yet. Indeed, the EYE-NEON study will assess the incidence and prevalence of NE-MNV, and the usefulness of NE-MNV as a predictor of exudation by analyzing OCTA at 2 years’ follow-up of fellow eyes of unilateral AMD [61]. Interestingly, Altinisk et al. found no significant differences in morphological features, area and activation findings of exudative type 1 MNV in nAMD and pachychoroid neovasculopathy, as well [62]. Although NE-MNV usually referred to type 1 MNV, other MNV subtypes could be identified as “non-exudative,” including the preclinical stage of type 3 MNV (“nascent type 3 MNV”; Fig. 3A) [49]. Though non-exudative MNV has usually been identified in the context of intermediate AMD, these lesions have been associated also with geographic atrophy (GA) [63]. Interestingly, OCTA sensitivity for detection of NE-MNV was significantly lower in GA than in intermediate AMD (~ 67% versus 82%, respectively), as a result of RPE and CC loss [63, 64]. Furthermore, OCTA nicely reported different morphological features of non-exudative lesions in these AMD stages. In detail, GA-associated NE MNV showed large neovascular trunks with no tortuosity and no capillaries, whereas in intermediate AMD these abnormalities displayed small

anastomotic vessels with a high capillary rate and increased tortuosity. Interestingly, this different morphology may reflect a dissimilar process of NE-MNV development (arteriogenesis in GA versus angiogenesis in intermediate AMD) [49, 63]. Importantly, treatment of these neovascular lesions in geographic atrophy should be reserved only to exudative MNV, due to the protective role of non-exudative neovessels in delaying the progression of atrophy [65–67].

EXUDATIVE MACULAR NEOVASCULARIZATION

A Focus on Type 1 MNV

Tangle, medusa, sea-fan, and dead tree (unclassified) are some vascular configurations of type 1 MNV that have been documented through OCTA [59, 68–70]. In detail, “tangle” MNV was associated with rosette-like capillaries with regular branching but no obvious feeder vessels [59]. “Medusa” neovascularization consists of tiny vessels radiating in all directions from a central feeder vessel [68]. In “sea-fan” morphology, 90% of pathologic vessels spreads from a peripheral feeder vessel with no main vessel trunk identifiable [69]. The “glomerulus” shape resembles the structure of a nephron and is composed of numerous, well defined, round, fine, and dense vessels [70]. Finally, in “dead tree” or “unclassified” conformation, linear enlarged vessels of unknown type have been associated with fibrotic or atrophic disciform lesion [59, 70]. These angiographic patterns have been also classified as immature (tangle MNV), mature (medusa, and sea-fan MNV), and hypermature (dead tree MNV), and correlated to entity of growth and response to anti-vascular endothelial growth factor (VEGF) intravitreal injections. Immature forms were commonly MNV that were at high risk of growth and that were treatment-naïve, whereas sea-fan and hypermature cases displayed a moderate progression and a resistance to anti-angiogenic intravitreal therapy [59, 68]. Interestingly, polypoidal choroidal vasculopathy (PCV) displayed different OCTA patterns. This

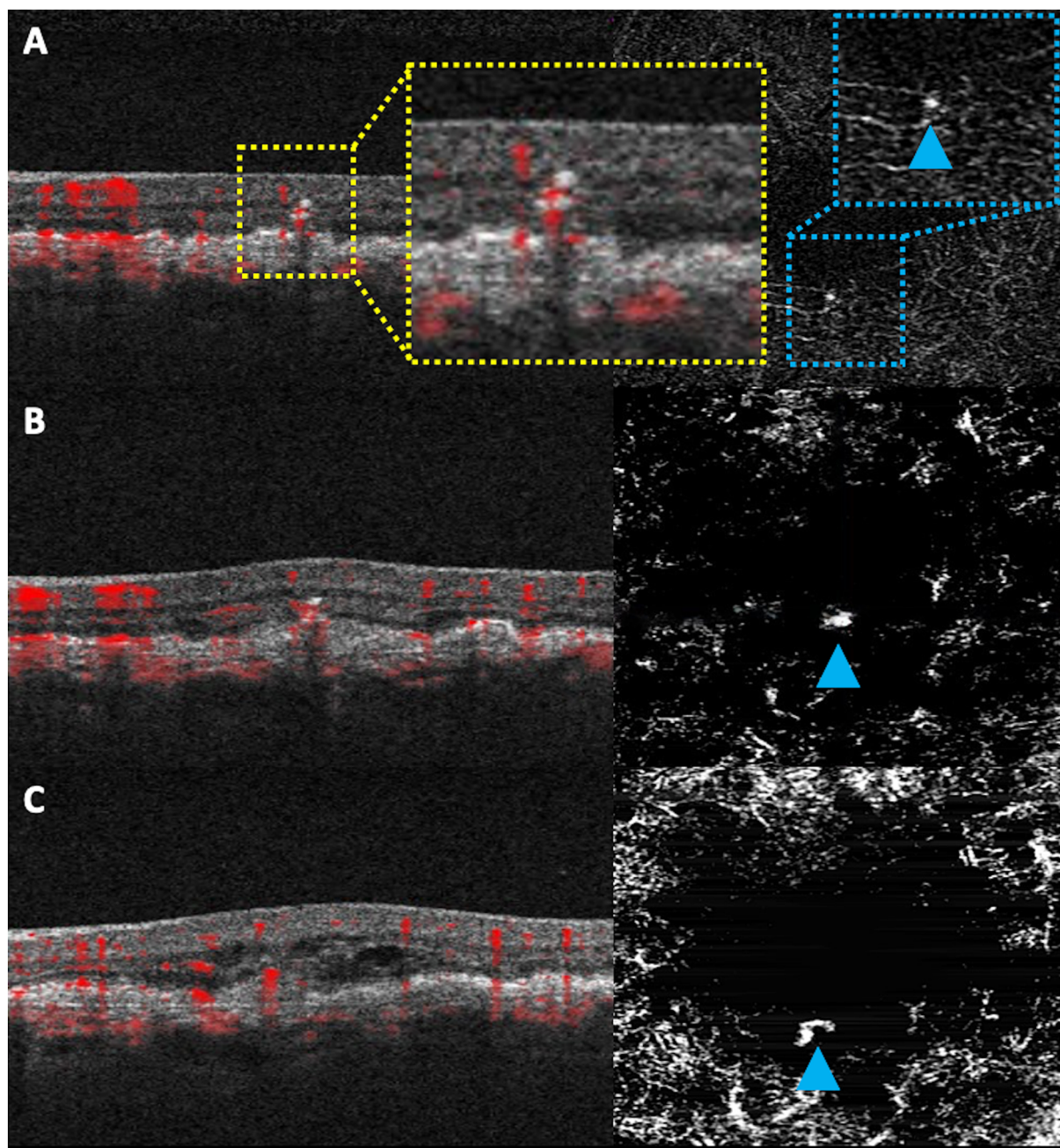


Fig. 3 (A–C) Optical coherence tomography angiography (OCTA) of a 71-year-old female patient affected by type 3 macular neovascularization (T3 MNV) in the fellow eye of a unilateral T3 MNV. **A** Baseline OCTA B-scan (left) and en-face (right) at deep capillary plexus level. Intraretinal hyperreflective foci (HRF) show detectable flow with no exudation, representing preclinical stage of T3 MNV (nascent T3 MNV), and overlay confluent pigment epithelium detachments (DEPs) with no contact with retinal pigment epithelium (RPE). Yellow panel: B-scan

magnification. Blue panel: en-face magnification, with a blue arrow indicating pathological vascular network. **(B)** 3-month follow-up OCTA B-scan (left) and en-face (right) at RPE level. HRF has grown toward RPE space and connected to DEP, developing exudative signs of overt MNV (blue arrow). **(C)** 6-month follow-up OCTA B-scan (left) and en-face (right) at retinal pigment epithelium (RPE) level. T3 neovascularization (blue arrow) displays evident signs of activation (intraretinal cysts)

neovascular lesion is characterized by nodular vascular agglomeration (polyp) and a branching vascular network (BVN) located in the sub-RPE [71]. It should be noted that PCV etiopathogenesis may arise from a spectrum of conditions, such as pachychoroid-related disease and nAMD. Chang and associates divided PCV into pachychoroid and non-pachychoroid groups with similar morphological features but distinct incidence. The pachychoroid phenotype displayed younger age of presentation, more pachychoroid disease features (e.g., pachychoroid, pachyvessels, pachydrusen), frequent large subretinal hemorrhages, and worse response to anti-VEGF treatment. On the contrary, non-pachychoroid PCV presented with older age, more nAMD characteristics (e.g., soft drusen), and fewer subretinal hemorrhages [72]. Interestingly, this phenotypic diversity may reflect the ethnicity of the population considered, despite this morphologic variation having not been related to genetic background [73]. Asian patients accounted for a PCV phenotype similar to pachychoroid neovascularopathy, whereas in the Caucasian population PCV may be thought as a subset of nAMD [74]. Since OCTA has reported variable sensitivity and specificity in detecting PCV, indocyanine green angiography is still regarded as the diagnostic gold standard. While BVN detection is similar or superior to ICGA, the aneurysmal lesion may be unnoticed by OCTA in the case of slow flow filling the polyp [75]. Interestingly, OCTA described different vascular patterns of BVN. Briefly, in the “trunk” configuration, central major vessels (trunk) extend toward the periphery through radiating branches. Similar to nephron glomeruli, “glomeruli” morphology was characterized by highly intersected vessels, whereas a “stick” pattern presented a small vascular network with no feeding vessels. Notably, glomeruli and stick morphologies had a greater recurrence rate; the latter was more prevalent in pachychoroid PCV [76]. Although PCV was typically thought of as a type 1 MNV variant with saccular or fusiform dilatations (and thus named “aneurysmal type 1 neovascularization”) [49], PCV could take on a structure analogous to type 2 MNV, with tangle vessels connecting to BVN. This pattern may be

considered a subtype or fruste form of PCV with no aneurysmatic polypoidal degeneration [77]. Furthermore, OCTA was employed to distinguish between PCV and nAMD. However, controversial OCTA sensitivity was reported, on the basis of scans used (43.9% in en-face slabs versus 82.6% cross-sectional images). This disparity could be explained by a distinct location for BVN and polyp, as well as a more imprecise segmentation of polyps by en-face slabs [78, 79]. However, a branch vascular network corresponded to a choriocapillaris hyper flow lesion, whereas a polypoidal lesion appeared either as a hypo flow or as a hyper flow round abnormality surrounded by a hypointense halo [80, 81].

A FOCUS ON TYPE 3 MNV

As mentioned before, OCTA significantly expanded our knowledge of type 3 MNV pathophysiology [1, 64–67]. This technology definitely demonstrated its intraretinal origin from deep vascular complex (DVC), which frequently denotes the complex of MCP and DCP [9], and the consequent events leading to its development. In brief, Sacconi et al. demonstrated that its preclinical stage (“nascent type 3 MNV”) represents an intraretinal vascular proliferation, and appears as hyperreflective foci (HFR) typically located between outer nuclear layer (ONL) and inner nuclear layer (INL) with detectable flow on OCTA, but with no exudation or contact with RPE. Subsequently, this preclinical lesion may grow from DVC toward sub-RPE space, and thereafter exudate (in the case of contact with RPE) or, more rarely, regress without other manifestations [82]. Recently, the same work group investigated the association between nascent GA and the onset of exudative type 3 MNV. Nascent GA corresponds to the subsidence of the outer plexiform layer (OPL) and INL, and to a hyporeflexive wedge-shaped band within OPL on structural OCT. From its original description, this finding represents a predictor of drusen-associated atrophy onset, although its association with type 3 MNV has been only hypothesized in the same study [86]. Interestingly, Sacconi and colleagues demonstrated how nascent GA precedes the

subsequent development in the same site of exudative type 3 MNV in about 23% of cases after 9 ± 6 months from atrophy onset [84]. The correlation between outer retinal and RPE atrophy and activation of this lesion has been described already [67, 87]. Notably, the RPE defect may be filled by adjacent RPE cells in the case of HRF, or by nascent GA if this RPE alteration is too extended. Since the risk of progression to an active type 3 is higher in the first year, the authors suggested a close 1-year surveillance to early detect not only atrophy but also exudative neovascularization, and to promptly start treatment [84]. In addition, OCT angiography supported the role of choriocapillaris ischemia in the development of type 3 MNV in affected eyes, but also in the fellow eyes [83, 85]. Indeed, patients with unilateral type 3 neovascularization have been frequently shown to develop an exudative type 3 MNV in the contralateral eye over a 3-year follow-up (60–100%) [88–92]. Similarly, our group reported a high cumulative incidence of exudative type 3 MNV (79%) by using OCTA (Fig. 3A–C). In detail, 58% of these patients showed a non-exudative form before, although with different onset. In fact, while 37% of cases presented this subclinical stage at baseline, for 21% of patients its development required an interval of time (13 ± 9 months). Interestingly, the onset of exudation was the shortest in the group of patients with a non-exudative neovascularization from baseline (9 ± 9 months). Alternatively, fellow eyes of unilateral type 3 MNV may proceed directly to an active form (21%) with no preclinical stage, or to GA (21%). Identification of non-exudative type 3 MNV on OCTA may be regarded as the earliest risk factor for an exudative form. Therefore, fellow eyes with this neovascular lesion should require a serial follow-up and a prompt treatment in the case of activation [85].

FUTURE APPLICATION: ARTIFICIAL INTELLIGENCE

Deep learning has gained a lot of attention as the most innovative artificial intelligence (AI)-method for analyzing images in several areas of

medicine. Through multiple levels of abstraction, DL systems make predictions from data that has been supplied into a training phase. Deep learning technology basically consists of two parts, including the technical networks (“brain”) and the datasets (“dictionary”). Convolutional neural network (CNN) is the most widely used network architecture. Similar to human visual cortex, CNN consists of multiple processing layers that associate the input volume (imaging acquisition) with a diagnostic output throughout differentiable functions. Interestingly, OCT-deep-learning-based models have been employed in AMD for its detection and differentiation from other maculopathies, the classification of its stages through biomarkers, and the prognostic evaluation (e.g., conversion to exudative form, response to anti-vascular endothelial growth factor). However, the analysis of these studies were beyond the scope of the present review [93, 94].

DL systems have also been applied to improve the data accessible for OCTA analysis. Since these algorithms could differentiate between flow and static voxels using any statistics (not only motion contrast), DL have been used to create de-novo OCTA scans from OCT images. Furthermore, CNN may improve the resolution of already collected OCTA scans. One additional application of deep learning is the removal of OCTA artifacts, including bulk motion and shadowing artifacts. Notably, the latter is particularly challenging since severe signal attenuation may totally interrupt reflectance signal. The most effective strategy is to carefully detect shadowing-affected regions to avoid the erroneous identification of non-perfusion areas (NPA) [32]. Notably, a DL algorithm can be utilized to overcome some OCTA limitations. By integrating data from other imaging modalities (e.g., OCT, color fundus photography), the DL system managed to distinguish an artery from a vein on OCTA scans [95]. NPA, macular neovascularization, and retinal fluid are a few examples of structural findings that learning-based technology has properly recognized and quantified, thus solving those imaging technical problems needing potent software solutions [32]. MNV, for instance, may be underestimated as a result of signal attenuation

and projection errors, or it may be misinterpreted as non-MNV pathology that is included in the segmentation result (e.g., drusen). Errors can also be associated with low contrast between neovascularization vessels and the background signal, requiring time-consuming review of images [96]. Recently, DL systems incorporated OCTA into the model training for computer-aided diagnosis (CAD) of retinal diseases, including AMD [96–100]. Recently, Wang and colleagues proposed a CNN-based model by using OCTA real-world multicenter dataset for MNV diagnosis and segmentation in AMD and non-AMD pathologies. This work group reported an overall accuracy of 95%, regardless of retinal disease.

Interestingly, better resolution images (3×3 mm scans) reported a higher accuracy, as compared with 6×6 mm slabs (99% versus 90%, respectively). Conversely, small scans could not capture the whole neovascular lesion. On the other hand, 6×6 mm scans typically reported reduced signal-to-noise ratio and an increased rate of artifacts. Furthermore, this model effectively evaluated MNV progression, as a rising number of pixels in correspondence of neovascularization could predict its exudation [96]. Notably, several multimodal imaging DL models also including OCTA have been proposed. In detail, Thakoor and associates differentiated AMD from other retinal disease by an OCT and OCTA CNN-based algorithm [97]. Similarly, Jin et al. assessed conversion to neovascular AMD (nAMD) with an accuracy (95.5%) comparable or even higher than those of retinal specialists [98]. However, the evaluation of MNV activity was based on presence of fluid, as compared with Vali et al., who independently evaluated MNV features by Coscas et al. [101] through a DL system [99]. Notably, the ONTARIO study by Sodhi and coworkers assessed the predictive ability of OCTA DL technology to determine long-term best-corrected visual acuity (BCVA) in nAMD. In detail, SS-OCT fluid metrics correlated with 1-year BCVA changes and was strengthened by complementary information from OCTA, providing a tool to personalize therapy and predict visual outcomes [100, 102]].

CONCLUSION

Despite its significant advantages, OCTA has not been employed in clinical practice as a gold standard diagnostic techniques yet, with the exception of contraindication to traditional angiography. Therefore, OCT angiography is still regarded as a complementary approach to conventional dye-based angiography.

Some obstacles to its universal use include inadequate visualization of slow blood-flow lesions, artifacts (e.g., projection artifacts), and a restricted field of view of the retinal periphery. However, post-processing algorithms (e.g., PR-OCTA, sacPR-OCTA, deep learning) applied to OCTA have mostly overcome part of these limitations, improving the quality of OCTA analysis. OCT angiography has meaningfully revolutionized our knowledge about nAMD, by introducing new clinical entities such as NE-MNV, and consolidating our pathophysiological comprehension of PCV and type 3 MNV. New technological development (e.g., 3D OCTA, artificial intelligence) has significantly enhanced OCTA detection rate, and provided new tools to assess and personalize therapeutic management.

Authors Contributions. Conceptualization: Giuseppe Querques; writing—original draft preparation: Beatrice Tombolini; writing—review and editing: Emanuele Crincoli, Riccardo Sacconi, and Marco Battista; literature search and data analysis: Federico Fantaguzzi and Andrea Servillo; and supervision: Francesco Bandello and Giuseppe Querques.

Funding. No funding or sponsorship was received for this study or publication of this article.

Declarations

Conflict of Interest. Beatrice Tombolini, Emanuele Crincoli, Marco Battista, Federico Fantaguzzi, and Andrea Servillo have nothing to disclose. Riccardo Sacconi has the following disclosures: Abbvie, Bayer, Medivis, Novartis, Roche, and Zeiss. Francesco Bandello has the

following disclosures: Allergan, Bayer, Boehringer-Ingelheim, Fidia Sooft, Hofmann La Roche, Novartis, Ntc Pharma, Sifi, Thrombogenics, and Zeiss. Giuseppe Querques has the following disclosures: Alimera Sciences, Allergan Inc, Amgen, Heidelberg, KBH, LEH Pharma, Lumithera, Novartis, Bayer Shering-Pharma, Sandoz, Sifi, Soof-Fidia, and Zeiss.

Ethical Approval. This article is based on previously conducted studies and does not contain any new studies with human participants or animals performed by any of the authors. Thus no approval from local ethics committee was required.

Open Access. This article is licensed under a Creative Commons Attribution-NonCommercial 4.0 International License, which permits any non-commercial use, sharing, adaptation, distribution and reproduction in any medium or format, as long as you give appropriate credit to the original author(s) and the source, provide a link to the Creative Commons licence, and indicate if changes were made. The images or other third party material in this article are included in the article's Creative Commons licence, unless indicated otherwise in a credit line to the material. If material is not included in the article's Creative Commons licence and your intended use is not permitted by statutory regulation or exceeds the permitted use, you will need to obtain permission directly from the copyright holder. To view a copy of this licence, visit <http://creativecommons.org/licenses/by-nc/4.0/>.

REFERENCES

- Spaide RF, Fujimoto JG, Waheed NK, Sadda SR, Staurengi G. Optical coherence tomography angiography. *Prog Retin Eye Res.* 2018;64:1–55.
- Borrelli E, Sarraf D, Freund KB, Sadda SR. OCT angiography and evaluation of the choroid and choroidal vascular disorders. *Prog Retin Eye Res.* 2018;67:30–55.
- Borrelli E, Sadda SVR, Uji A, Querques G. Pearls and pitfalls of optical coherence tomography angiography imaging: a review. *Ophthalmol Ther.* 2019;8(2):215–26.
- Borrelli E, Sadda SR, Uji A, Querques G. OCT angiography: guidelines for analysis and interpretation. In: *OCT and Imaging in Central Nervous System Diseases: The Eye as a Window to the Brain: Second Edition.* 2020.
- Borrelli E, Parravano M, Sacconi R, Costanzo E, Querques L, Vella G, et al. Guidelines on Optical Coherence Tomography Angiography Imaging: 2020 focused update. *Ophthalmol Ther.* 2020;9(4):697–707.
- Tombolini B, Borrelli E, Sacconi R, Bandello F, Querques G. Diabetic macular ischemia. *Acta Diabetol.* 2022;59(6):751–9.
- Rabiolo A, Carnevali A, Bandello F, Querques G. Optical coherence tomography angiography: evolution or revolution? *Expert Rev Ophthalmol.* 2016;11(4):243–5.
- Carnevali A, Mastropasqua R, Gatti V, Vaccaro S, Mancini A, D'aloisio R, et al. Optical coherence tomography angiography in intermediate and late age-related macular degeneration: review of current technical aspects and applications. *Appl Sci.* 2020;10(24):1–20.
- Campbell JP, Zhang M, Hwang TS, Bailey ST, Wilson DJ, Jia Y, et al. Detailed vascular anatomy of the human retina by projection-resolved optical coherence tomography angiography. *Sci Rep.* 2017;7:1–11.
- Bjerager J, Schneider M, Potapenko I, Van Dijk EHC, Faber C, Grauslund J, et al. Diagnostic accuracy of the Amsler grid test for detecting neovascular age-related macular degeneration: a systematic review and meta-analysis. *JAMA Ophthalmol.* 2023;141(4):315–23.
- Brucker J, Bhatia V, Sahel JA, Girmens JF, Mohand-Saïd S. Odysight: a mobile medical application designed for remote monitoring—a prospective study comparison with standard clinical eye tests. *Ophthalmol Ther.* 2019;8(3):461–76.
- Láins I, Wang JC, Cui Y, Katz R, Vingopoulos F, Staurengi G, et al. Retinal applications of swept source optical coherence tomography (OCT) and optical coherence tomography angiography (OCTA). *Prog Retin Eye Res.* 2021;84:100951.
- Rogowska J. Overview and Fundamentals of Medical Image Segmentation. *Handbook of Medical Imaging.* Academic Press; 2000. 69–85

14. Durbin MK, An L, Shemonski ND, Soares M, Santos T, Lopes M, et al. Quantification of retinal microvascular density in optical coherence tomographic angiography images in diabetic retinopathy. *JAMA Ophthalmol*. 2017;135(4):370–6.
15. Corvi F, Pellegrini M, Erba S, Cozzi M, Staurenghi G, Giani A. Reproducibility of vessel density, fractal dimension, and foveal avascular zone using 7 different optical coherence tomography angiography devices. *Am J Ophthalmol*. 2018;1(186):25–31.
16. Rabiolo A, Gelormini F, Marchese A, Cicinelli MV, Triolo G, Sacconi R, et al. Macular perfusion parameters in different angiocube sizes: does the size matter in quantitative optical coherence tomography angiography? *Investig Ophthalmol Vis Sci*. 2018;59(1):231–7.
17. Rabiolo A, Gelormini F, Sacconi R, Cicinelli MV, Triolo G, Bettin P, et al. Comparison of methods to quantify macular and peripapillary vessel density in optical coherence tomography angiography. *PLoS ONE*. 2018;13(10):1–20.
18. Mehta N, Liu K, Alibhai AY, Gendelman I, Braun PX, Ishibazawa A, et al. Impact of binarization thresholding and brightness/contrast adjustment methodology on optical coherence tomography angiography image quantification. *Am J Ophthalmol*. 2019;205:54–65.
19. Sacconi R, Borrelli E, Corbelli E, Capone L, Rabiolo A, Carnevali A, et al. Quantitative changes in the ageing choriocapillaris as measured by swept source optical coherence tomography angiography. *Br J Ophthalmol*. 2019;103(9):1320–6.
20. Borrelli E, Souied EH, Freund KB, Querques G, Miere A, Gal-Or O, et al. Reduced choriocapillaris flow in eyes with type 3 neovascularization and age-related macular degeneration. *Retina*. 2018;38(10):1968–76.
21. Chu Z, Cheng Y, Zhang Q, Zhou H, Dai Y, Shi Y, et al. Quantification of choriocapillaris with phansalkar local thresholding: pitfalls to avoid. *Am J Ophthalmol*. 2020;1(213):161–76.
22. Meira J, Marques ML, Falcão-Reis F, Gomes ER, Carneiro Â. Immediate reactions to fluorescein and indocyanine green in retinal angiography: review of literature and proposal for patient's evaluation. *Clin Ophthalmol*. 2020;14:171–8.
23. Jia Y, Tan O, Tokayer J, Potsaid B, Wang Y, Liu JJ, et al. Split-spectrum amplitude-decorrelation angiography with optical coherence tomography. *Opt Express*. 2012;20(4):4710–25.
24. Uji A, Balasubramanian S, Lei J, Baghdasaryan E, Al-Sheikh M, Sadda SR. Impact of multiple en face image averaging on quantitative assessment from optical coherence tomography angiography images. *Ophthalmology*. 2017;124(7):944–52.
25. Spaide RF, Fujimoto JG, Waheed NK. Image artifacts in optical coherence tomography angiography. *Retina*. 2015;35(11):2163–80.
26. Anvari P, Ashrafkhorasani M, Habibi A, Falavarjani KG. Artifacts in optical coherence tomography angiography. *J Ophthalmic Vis Res*. 2021;16(2):271–86.
27. Ghasemi Falavarjani K, Al-Sheikh M, Akil H, Sadda SR. Image artefacts in swept-source optical coherence tomography angiography. *Br J Ophthalmol*. 2017;101(5):564–8.
28. Ghasemi Falavarjani K, Habibi A, Anvari P, Ghasemizadeh S, Ashraf Khorasani M, Shenazandi H, et al. Effect of segmentation error correction on optical coherence tomography angiography measurements in healthy subjects and diabetic macular oedema. *Br J Ophthalmol*. 2020;104(2):162.
29. Wang J, Hormel TT, Gao L, Zang P, Guo Y, Wang X, et al. Automated diagnosis and segmentation of choroidal neovascularization in OCT angiography using deep learning. *Biomed Opt Express*. 2020;11(2):927–44.
30. Hormel TT, Huang D, Jia Y. Artifacts and artifact removal in optical coherence tomographic angiography. *Quant Imaging Med Surg*. 2021;11(3):1120–33.
31. Ang JIEW, Ormel TRTH, Ailey STTB, Wang THSH, Uang DAH, Ia YALIJ. Signal attenuation-compensated projection-resolved OCT angiography. *Prog Retin Eye Res*. 2023;14(5):2040–54
32. Hormel TT, Hwang TS, Bailey ST, Wilson DJ, Huang D, Jia Y. Artificial intelligence in OCT angiography. *Prog Retin Eye Res*. 2021;85:1–63.
33. Arrigo A, Aragona E, Battaglia Parodi M, Bandello F. Quantitative approaches in multimodal fundus imaging: state of the art and future perspectives. *Prog Retin Eye Res*. 2022;2023(92): 101111.
34. Sekiryu T. Choroidal imaging using optical coherence tomography: techniques and interpretations. *Jpn J Ophthalmol*. 2022;66(3):213–26.
35. Choi W, Mohler KJ, Potsaid B, Lu CD, Liu JJ, Jayaraman V, et al. Choriocapillaris and choroidal microvasculature imaging with ultrahigh speed OCT angiography. *PLoS ONE*. 2013;8(12): e81499.
36. Poddar R, Migacz JV, Schwartz DM, Werner JS, Gorczyńska I. Challenges and advantages in wide-field optical coherence tomography angiography

- imaging of the human retinal and choroidal vasculature at 1.7-MHz A-scan rate. *J Biomed Opt.* 2017;22(10):1–14.
37. Borrelli E, Sacconi R, Brambati M, Bandello F, Querques G. In vivo rotational three-dimensional OCTA analysis of microaneurysms in the human diabetic retina. *Sci Rep.* 2019;9(1)
 38. Borrelli E, Sacconi R, Klose G, de Sisternes L, Bandello F, Querques G. Rotational three-dimensional OCTA: a notable new imaging tool to characterize type 3 macular neovascularization. *Sci Rep.* 2019;9(1).
 39. Breazzano MP, Bacci T, Curcio CA, Freund K. Novel multimodal imaging and volume rendering of type 3 macular neovascularization. *Retina.* 2020;40:e55–57.
 40. Borrelli E, Mastropasqua L, Souied E, Sadda SV, Vella G, Toto L, et al. Longitudinal assessment of type 3 macular neovascularization using 3D volume-rendering OCTA. *Can J Ophthalmol.* 2022;57(4):228–235.
 41. Borrelli E, Sacconi R, Querques L, Battista M, Bandello F, Querques G. Quantification of diabetic macular ischemia using novel three-dimensional optical coherence tomography angiography metrics. *J Biophotonics.* 2020;13(10):885–891.
 42. Borrelli E, Parravano M, Costanzo E, Sacconi R, Querques L, Pennisi F, et al. Using three-dimensional optical coherence tomography angiography metrics improves repeatability on quantification of ischemia in eyes with diabetic macular edema. *Retina.* 2021;41(8):1660–7.
 43. Kalaw FGP, Alex V, Walker E, Bartsch D-U, Freeman WR, Borooah S. Inner retinal thickness and vasculature in patients with reticular pseudodrusen. *Ophthalmic Res.* 2023;1:885–91.
 44. Wei Y-Z, Huang H, Zhang X, Yu H-H, Liu B-Y, Diao Y-Y, et al. Identification of retinal thickness and blood flow in age-related macular degeneration with reticular pseudodrusen. *Int J Ophthalmol.* 2023;16(8):1268–73.
 45. Li J, Liu Z, Lu J, Shen M, Cheng Y, Siddiqui N, et al. Decreased macular choriocapillaris perfusion in eyes with macular reticular pseudodrusen imaged with swept-source OCT angiography. *Invest Ophthalmol Vis Sci.* 2023;64(4):15.
 46. Abdolrahimzadeh S, Zweifel SA, Di Pippo M, Bajka A, Scuderi G, Lotery AJ. Central macular choriocapillaris impairment as a manifestation of microvascular disease in eyes with subretinal drusenoid deposits. *Eye (Lond).* 2023;
 47. Wu Z, Zhou X, Chu Z, Gregori G, Wang RK, Rosenfeld PJ, et al. Impact of reticular pseudodrusen on choriocapillaris flow deficits and choroidal structure on optical coherence tomography angiography. *Invest Ophthalmol Vis Sci.* 2022;63(12):1.
 48. Querques G, Srouf M, Massamba N, Georges A, Ben Moussa N, Rafaeli O, et al. Functional characterization and multimodal imaging of treatment-naïve “quiescent” choroidal neovascularization. *Invest Ophthalmol Vis Sci.* 2013;54(10):6886–92.
 49. Sacconi R, Fragiotta S, Sarraf D, Sadda SVR, Freund KB, Parravano M, et al. Towards a better understanding of non-exudative choroidal and macular neovascularization. *Prog Retin Eye Res.* 2022;2022(92): 101113.
 50. Greenberg JR, Kim BY, Brady CJ, Millay RH, Raut R. Optical coherence tomography angiography for detecting nonexudative macular neovascularization in age-related macular degeneration. *J Vitreoretin Dis.* 2023;7(1):16–9.
 51. Stattin M, Ahmed D, Haas A-M, Graf A, Zehetner C, Mihalics S, et al. Optical coherence tomography and OCT angiography characteristics of indocyanine green angiographic plaques in nonexudative age-related macular degeneration. *Retina.* 2023;43(1):16–24.
 52. Siggel R, Spital C, Lentzsch A, Liakopoulos S. Optical coherence tomography angiography for the detection of macular neovascularization-comparison of en face versus cross-sectional view. *Eye (Lond).* 2023;37(2):256–62.
 53. Querques G, Sacconi R, Capuano V, Carnevali A, Colantuono D, Battista M, et al. Treatment-naïve quiescent macular neovascularization secondary to AMD: The 2019 Young Investigator Lecture of Macula Society. *Eur J Ophthalmol.* 2021;31(6):3164–76.
 54. Carnevali A, Sacconi R, Querques L, Marchese A, Capuano V, Rabiolo A, et al. Natural history of treatment-naïve quiescent choroidal neovascularization in age-related macular degeneration using OCT angiography. *Ophthalmol Retina.* 2018;2(9):922–30.
 55. Teo KYC, Yanagi Y, Wong TY, Charkravarty U, Cheung CMG. Morphologic predictors and temporal characteristics of conversion from nonexudative to exudative age-related macular degeneration in the fellow eye. *Ophthalmol Retina.* 2021;5(2):126–40.
 56. Solecki L, Loganadane P, Gauthier A-S, Simonin M, Puyraveau M, Delbosc B, et al. Predictive factors for exudation of quiescent choroidal neovessels

- detected by OCT angiography in the fellow eyes of eyes treated for a neovascular age-related macular degeneration. *Eye*. 2021;35(2):644–50.
57. Fragiotta S, Parravano M, Costanzo E, De Geronimo D, Varano M, Fernández-Avellaneda P, et al. Subretinal lipid globules an early biomarker of macular neovascularization in eyes with intermediate age-related macular degeneration. *Retina*. 2023;43:913.
 58. Wang Y, Sun J, Wu J, Jia H, Feng J, Chen J, et al. Growth of nonexudative macular neovascularization in age-related macular degeneration: an indicator of biological lesion activity. *Eye (Lond)*. 2023;37(10):2048–54.
 59. Xu D, Dávila JP, Rahimi M, Rebhun CB, Alibhai AY, Waheed NK, et al. Long-term progression of type 1 neovascularization in age-related macular degeneration using optical coherence tomography angiography. *Am J Ophthalmol*. 2018;187:10–20.
 60. Maltsev DS, Kulikov AN, Perminova SM, Burnasheva MA, Vasiliev AS. Multimodal Imaging in non-exudative choroidal neovascularization: a pilot study of status of retinal pigment epithelium. *Retina*. 2023;43:2019.
 61. Thottarath S, Chandra S, Gurudas S, Tsai W-S, Giani A, De Cock E, et al. Study protocol on prevalence of non-exudative macular neovascularisation and its contribution to prediction of exudation in fellow eyes with unilateral exudative AMD (EYE-NEON). *Eye (Lond)*. 2023;37:3004.
 62. Altinisik M, Kurt E, Sonmezer P, Kayikcioglu O, Ilker SS. A comparative study of type 1 neovascularization: neovascular age-related macular degeneration versus pachychoroid neovascularopathy. *Eur J Ophthalmol*. 2022;32(4):2404–11.
 63. Capuano V, Miere A, Querques L, Sacconi R, Carnevali A, Amoroso F, et al. Treatment-naïve quiescent choroidal neovascularization in geographic atrophy secondary to nonexudative age-related macular degeneration. *Am J Ophthalmol*. 2017;182:45–55.
 64. Carnevali A, Cicinelli MV, Capuano V, Corvi F, Mazzaferro A, Querques L, et al. Optical coherence tomography angiography: a useful tool for diagnosis of treatment-naïve quiescent choroidal neovascularization. *Am J Ophthalmol*. 2016;169:189–98.
 65. Heiferman MJ, Fawzi AA. Progression of subclinical choroidal neovascularization in age-related macular degeneration. *PLoS ONE*. 2019;14(6): e0217805.
 66. Pfau M, Möller PT, Künzel SH, von der Emde L, Lindner M, Thiele S, et al. Type 1 choroidal neovascularization is associated with reduced localized progression of atrophy in age-related macular degeneration. *Ophthalmol Retin*. 2020;4(3):238–48.
 67. Sacconi R, Brambati M, Miere A, Costanzo E, Capuano V, Borrelli E, et al. Characterisation of macular neovascularisation in geographic atrophy. *Br J Ophthalmol*. 2022;106(9):1282–7.
 68. Barayev E, Meshi A, Gershoni A, Segal O, Dotan A, Hadayer A, et al. Optical coherence tomography angiography patterns of type 1 macular neovascularization in age-related macular degeneration patients. *Eur J Ophthalmol*. 2023;33(4):1697–705.
 69. Kuehlewein L, Bansal M, Lenis TL, Iafe NA, Satta SR, Bonini Filho MA, et al. Optical coherence tomography angiography of type 1 neovascularization in age-related macular degeneration. *Am J Ophthalmol*. 2015;160(4):739–748.e2.
 70. Ahmed M, Syrine BM, Nadia BA, Anis M, Karim Z, Mohamed G, et al. Optical coherence tomography angiography features of macular neovascularization in wet age-related macular degeneration: a cross-sectional study. *Ann Med Surg*. 2021;70: 102826.
 71. Cheung CMG, Lai TYY, Ruamviboonsuk P, Chen S-J, Chen Y, Freund KB, et al. Polypoidal choroidal vasculopathy: definition, pathogenesis, diagnosis, and management. *Ophthalmology*. 2018;125(5): 708–24.
 72. Chang YC, Cheng CK. Difference between pachychoroid and nonpachychoroid polypoidal choroidal vasculopathy and their response to anti-vascular endothelial growth factor therapy. *Retina*. 2020;40(7):1403–11.
 73. Simão JM, Farinha CV, Marques JP, Nunes S, Pires IM, Cachulo ML, et al. Polypoidal choroidal vasculopathy in Caucasians: morphological findings from multimodal retinal imaging. *Ophthalmol J Int d'ophtalmologie Int J Ophthalmol Zeitschrift fur Augenheilkd*. 2021;244(4):315–25.
 74. Corvi F, Chandra S, Invernizzi A, Pace L, Viola F, Sivaprasad S, et al. Multimodal imaging comparison of polypoidal choroidal vasculopathy between Asian and Caucasian populations. *Am J Ophthalmol*. 2022;234:108–16.
 75. Fenner BJ, Cheung CMG, Sim SS, Lee WK, Staurenghi G, Lai TYY, et al. Evolving treatment paradigms for PCV. *Eye*. 2022;36(2):257–65.
 76. Huang C-H, Yeh P-T, Hsieh Y-T, Ho T-C, Yang C-M, Yang C-H. Characterizing branching vascular network morphology in polypoidal choroidal vasculopathy by optical coherence tomography angiography. *Sci Rep*. 2019;9(1):595.

77. Hua R, Duan J, Zhang M. Pachychoroid spectrum disease: underlying pathology, classification, and phenotypes. *Curr Eye Res.* 2021;46(10):1437–48.
78. De Carlo TE, Kokame GT, Kaneko KN, Lian R, Lai JC, Wee R. Sensitivity and specificity of detecting polypoidal choroidal vasculopathy with en face optical coherence tomography and optical coherence tomography angiography. *Retina.* 2019;39(7):1343.
79. Cheung CMG, Yanagi Y, Akiba M, Tan A, Mathur R, Chan CM, et al. Improved detection and diagnosis of polypoidal choroidal vasculopathy using a combination of optical coherence tomography and optical coherence tomography angiography. *Retina.* 2019;39(9):1655.
80. Inoue M, Balaratnasingam C, Freund KB. Optical coherence tomography angiography of polypoidal choroidal vasculopathy and polypoidal choroidal neovascularization. *Retina.* 2015;35(11):2265–74.
81. Srour M, Querques G, Semoun O, El AA, Miere A, Sikorav A, et al. Optical coherence tomography angiography characteristics of polypoidal choroidal vasculopathy. *Br J Ophthalmol.* 2016;100(11):1489–93.
82. Sacconi R, Sarraf D, Garrity S, Freund KB, Yannuzzi LA, Gal-Or O, et al. Nascent type 3 neovascularization in age-related macular degeneration. *Ophthalmol Retina.* 2018;2(11):1097–106.
83. Sacconi R, Forte P, Tombolini B, Grosso D, Fantaguzzi F, Pina A, et al. OCT predictors of 3-year visual outcome for type 3 macular neovascularization. *Ophthalmol Retin.* 2022;6(7):586–94.
84. Sacconi R, Sarraf D, Satta SR, Freund KB, Servillo A, Fogel Levin MM, et al. Nascent geographic atrophy as a predictor of type 3 macular neovascularization development. *Ophthalmol Retin.* 2023;7(7):586–92.
85. Sacconi R, Forte P, Capuano V, Miere A, Costanzo E, Tombolini B, et al. Optical coherence tomography angiography characterization of evolving lesions in fellow eyes of exudative type 3 macular neovascularization patients. *Retina.* 2022;42(11):2075–82.
86. Wu Z, Luu CD, Ayton LN, Goh JK, Lucci LM, Hubbard WC, et al. Optical coherence tomography-defined changes preceding the development of drusen-associated atrophy in age-related macular degeneration. *Ophthalmology.* 2014;121(12):2415–22.
87. Spaide RF. New proposal for the pathophysiology of type 3 neovascularization as based on multimodal imaging findings. *Retina.* 2019;39(8):1451.
88. Gross NE, Aizman A, Brucker A, Klancnik JMJ, Yannuzzi LA. Nature and risk of neovascularization in the fellow eye of patients with unilateral retinal angiomatous proliferation. *Retina.* 2005;25(6):713–8.
89. Sacconi R, Battista M, Borrelli E, Miere A, Corbelli E, Capuano V, et al. OCT-A characterisation of recurrent type 3 macular neovascularisation. *Br J Ophthalmol.* 2021;105(2):222–6.
90. Borrelli E, Sacconi R, Klose G, de Sisternes L, Bاندello F, Querques G. Rotational three-dimensional OCTA: a notable new imaging tool to characterize type 3 macular neovascularization. *Sci Rep.* 2019;9(1):1–8.
91. Campa C, Harding SP, Pearce IA, Beare NAV, Briggs MC, Heimann H. Incidence of neovascularization in the fellow eye of patients with unilateral retinal angiomatous proliferation. *Eye (Lond).* 2010;24(10):1585–9.
92. Sawa M, Ueno C, Gomi F, Nishida K. Incidence and characteristics of neovascularization in fellow eyes of Japanese patients with unilateral retinal angiomatous proliferation. *Retina.* 2014;34(4):761–7.
93. Koseoglu ND, Grzybowski A, Liu TYA. Deep learning applications to classification and detection of age-related macular degeneration on optical coherence tomography imaging: a review. *Ophthalmol Ther.* 2023;12:2347.
94. Paul SK, Pan I, Sobol WM. A systematic review of deep learning applications for optical coherence tomography in age-related macular degeneration. *Retina.* 2022;42(8):1417–24.
95. Alam M, Toslak D, Lim JI, Yao X. OCT feature analysis guided artery-vein differentiation in OCTA. *Biomed Opt Express.* 2019;10(4):2055.
96. Wang J, Hormel TT, Tsuboi K, Wang X, Ding X, Peng X, et al. Deep learning for diagnosing and segmenting choroidal neovascularization in OCT angiography in a large real-world data set. *Transl Vis Sci Technol.* 2023;12(4):1–14.
97. Thakoor KA, Yao J, Bordbar D, Moussa O, Lin W, Sajda P, et al. A multimodal deep learning system to distinguish late stages of AMD and to compare expert vs. AI ocular biomarkers. *Sci Rep.* 2022;12(1):1–11.
98. Jin K, Yan Y, Chen M, Wang J, Pan X, Liu X, et al. Multimodal deep learning with feature level fusion for identification of choroidal neovascularization activity in age-related macular degeneration. *Acta Ophthalmol.* 2022;100(2):e512–20.

-
99. Vali M, Nazari B, Sadri S, Pour EK, Riazi-Esfahani H, Faghihi H, et al. CNV-Net: segmentation, classification and activity score measurement of choroidal neovascularization (CNV) using optical coherence tomography angiography (OCTA). *Diagnostics*. 2023;13(7):1309.
 100. Sodhi SK, Pereira A, Oakley JD, Golding J, Trimboli C, Russakoff DB, et al. Utilization of deep learning to quantify fluid volume of neovascular age-related macular degeneration patients based on swept-source OCT imaging: the ONTARIO study. *PLoS ONE*. 2022;17(2):1–12.
 101. Coscas GJ, Lupidi M, Coscas F, Cagini C, Souied EH. Optical coherence tomography angiography versus traditional multimodal imaging in assessing the activity of exudative age-related macular degeneration: a new diagnostic challenge. *Retina*. 2015;35(11):2219–28.
 102. Donald J, Jallow S, Davis B. Adult vitelliform macular detachment occurring in patients with basal laminar drusen. *Am J Ophthalmol*. 1985;99(4):445–59.